Satellite Cells Are Activated In A Rat Model of Radiation-Induced Muscle Fibrosis

Xiaoling Zeng
University of South China
Luyuan Xie
Changsha Medical University
Yuxin Ge
University of South China
Yue Zhou
University of South China
Hui Wang
University of South China
Yongyi Chen
University of South China
Xiaomei Zhu
University of South China
Huayun Liu
University of South China
Qianjin Liao
University of South China
Yu Kong
Chinese Academy of Sciences Shanghai Advanced Research Institute
Lijun Pan
Chinese Academy of Sciences Shanghai Advanced Research Institute
Junjun Li
University of South China
Lei Xue
University of South China
Sha Li
University of South China
Xiao Zhou
University of South China
Chunmeng Shi
Third Military Medical College: Air Force Medical University
Xiaowu Sheng (shengxiaowu789@163.com)

University of South China https://orcid.org/0000-0002-0558-6616

Research

Keywords: Radiation, muscle

Posted Date: August 25th, 2021

DOI: https://doi.org/10.21203/rs.3.rs-826976/v1

Version of Record: A version of this preprint was published at Radiation Research on March 16th, 2022. See the published version at https://doi.org/10.1667/RADE-21-00183.1.

Abstract

Background: Radiation-induced muscle fibrosis is a long-term side effect of radiotherapy that significantly affect the quality of life and even reduces the survival of cancer patients. We have demonstrated that radiation induces satellite cell (SC) activation at the molecular level; however, cellular evidence in a rat model of radiation-induced muscle fibrosis was lacking. In this study, we evaluated SC activation *in vivo* and investigated whether radiation affects the proliferation and differentiation potential of SCs *in vitro*.

Methods: For *in vivo* studies, Sprague-Dawley rats were randomly divided into six groups (n = 6 per group): a non-irradiated control group and 90 Gy-1 w, 90 Gy-2 w, 90 Gy-4 w, 90 Gy-12 w, and 90 Gy-24 w groups.Left groin area of the rats received a single dose of irradiation and rectus femoris tissues were collected in the indicated weeks. Fibrosis, apoptosis, and autophagy were evaluated by Masson's trichrome staining, TUNEL staining, and electron microscopy, respectively. SC activation and central nuclear muscle fibers were evaluated by immunofluorescence staining and hematoxylin and eosin staining. IL-1β concentrations in serum and irradiated muscle tissue samples were determined by ELISA. For *in vitro* studies, SCs were isolated from rats with radiation-induced muscle fibrosis and their proliferation and differentiation were evaluated by immunofluorescence staining.

Results: *In vivo*, fibrosis increased over time following irradiation. Apoptosis and autophagy levels, IL-1β concentrations in serum and irradiated skin tissues, and the numbers of SCs and central nuclear muscle fibers were increased in the irradiated groups when compared with control group. *In vitro*, cultured SCs from irradiated muscle were positive for proliferation marker Pax7, and differentiated SCs were positive for myogenic differentiation marker MyHC.

Conclusion: This study provided cellular evidence of SC activation and proliferation in rats with radiation-induced muscle fibrosis. Radiation does not affect the proliferation and differentiation potential of SCs *in vitro*.

Introduction

Skeletal muscle is composed of multinucleated myocytes that are responsible for skeletal muscle contraction (1). Radiation-induced muscle fibrosis is a long-term side effect of radiotherapy with multiple symptoms, such as skeletal muscle weakness, dystonia, stiffness, and functional disorder, which can lead to local tissue hypoxia, scarring, and contraction, resulting in difficulty in re-operation for cancer recurrence and in poor efficacy of re-irradiation. It significantly affects the quality of life and even reduces the survival of cancer patients(2)

Muscle regeneration after injury is generally mediated by skeletal muscle satellite cells (SCs), which can be reactivated and migrate to the injured site, proliferate, and differentiate into new muscle cells to repair damaged muscles or maintain the stem cell bank(3, 4). In 1961, using electron microscopy, Mauro discovered that SCs are located on the surfaces of the muscle fibers between the myofiber plasma

lemma and the basal lamina in frogs(5). SCs are myogenic progenitors that can proliferate, differentiate, and self-renew *in vitro* and *in vivo*(6-8). In response to muscle injury, SCs are activated and re-enter the cell cycle for proliferation and myogenic differentiation, and then migrate to the injured site and fuse with the damaged muscle fibers to repair them or generate new muscle fibers. This process is characterized by time-regulated gene expression control. In the quiescent state, SCs express paired gene 7 (Pax7), but lack myogenic determination factor (MyoD). During myogenic differentiation, SCs start to express myogenic factor 5 (Myf5) protein and MyoD, followed by the terminal differentiation marker myogenin (MyoG) (9). Growth factors such as hepatocyte growth factor (HGF) and insulin-like growth factor I (IGF-I) participate in the activation, proliferation, differentiation, and migration of SCs during the repair process(10, 11). While in normal fibers, the nuclei are located at the cell periphery, in regenerated fibers, they are located in the center of the cells. Central nuclear muscle fibers are a hallmark of muscle regeneration (12).

As SCs are myogenic stem cells, several approaches to isolate SCs from different species, including rats(13) , mice(14), humans (15), chickens (16), pigs (17), and cows (18), have been reported. Ding et al. developed a method to isolate highly purified porcine SCs using fluorescence-activated cell sorting and found that long-term *in-vitro* culturing of the purified SCs led to stemness loss(19). In the absence of SCs, injured muscle is infiltrated with inflammatory cells and replaced by fat and fibrotic tissue (20). In our previous study, we found that radiation induces SC activation at the molecular level; however, cellular evidence of SC activation in a rat model of radiation-induced muscle fibrosis was lacking.

Radiation breaks the chemical bonds on the helical DNA backbone, causing direct or indirect DNA damage, which leads to cell death. Apoptosis is the primary mechanism of radiation-induced cell death. Autophagy is a self-degenerative process that is important in the removal of aggregated proteins, damaged organelles, and intracellular pathogens, and plays a role in preventing apoptosis (21). Furthermore, autophagy is required for skeletal muscle homeostasis and regeneration. Autophagy is indispensable in SC quiescence, activation, differentiation, and apoptosis(22). Quiescent SCs exhibit constitutive autophagic activity to maintain stemness(23). During the transition from quiescence to activation and differentiation, autophagy provides nutrients(24). During myoblast fusion to form myotubes, mitochondrial function and activity are greatly increased, which is accompanied by autophagy(24). Sirtuin 1 (SIRT1) has been identified as a critical regulator of autophagic flux and SC activation, and loss of SIRT1 results in disturbed autophagic activity and defective SC activation(25). Genetic deletion of autophagy-related protein 7 (ATG7) suppresses SC proliferation and differentiation and causes defective muscle regeneration(26). Based on these findings, we hypothesized that autophagy may play a role in radiation-induced muscle fibrosis.

To help resolve the above questions, we evaluated SC activation in rats with radiation-induced muscle fibrosis using morphological and biochemical methods. In addition, SCs isolated from the model rats were evaluated for their proliferation and differentiation potential *in vitro.* We expected this study to provide cytological evidence of SC activation as well as an experimental basis for activated SC-mediated muscle regeneration.

Materials And Methods

Experimental animals

Eight-week-old Sprague-Dawley rats from Hunan SJA Laboratory Animal Co., Ltd. (Hunan, China) were used in this study. All researchers were trained and qualified at Central South University prior to the operation. Housing conditions and animal manipulations were carried out in accordance with the Guidelines for the Care and Use of Laboratory Animals of Hunan Cancer Hospital and were reviewed and approved by the Animal Ethics Committee.

Establishment of a radiation-induced muscle fibrosis rat model and treatments

The rats had free access to food and water. They were allowed to adapt to the environment for 1 week and were then randomly divided into six groups (n = 6 per group): non-irradiated control, 90 Gy-1 w, 90 Gy-2 w, 90 Gy-4 w, 90 Gy-12 w, and 90 Gy-24 w groups. After the rats were anesthetized with 5% pentobarbital sodium, a single dose of 90Gy was administered according to a previously reported procedure (26),The irradiated area was the surface of the medial rectus femoris on the left thigh. In the 1st, 2nd, 4th, 12th, and 24th weeks after irradiation, animals from each group were sacrificed. Superficial muscle tissues were collected, and blood was collected from the heart. The blood was left standing at room temperature for 30–60 min, and serum was extracted by centrifugation at 3000 rpm for 10 min.

SC isolation and culturec

Cut the muscle into about $1m^3$ small particles and put them in the centrifuge tube, add PBS solution, stand for 5min, discard the supernatant, add 1ml type II collagenase solution (11088831001;Roche), mix well, incubate in a 37℃ constant temperature water bath for 15min, blow and shake the centrifuge tube with a straw every 5min, centrifuge at 1000r / min for 5min, discard the supernatant, Add 1ml of type II dispase enzyme solution (4942078001;Roche), mix well, incubate in a 37 ℃ constant temperature water bath for 15min, blow and shake the centrifuge tube with a straw every 5min or shake it gently for 1min, centrifuge at 1000r / min for 5min, discard the supernatant, add 1ml of 0.25% trypsin solution, mix well, and incubate in a 37 ℃ constant temperature water bath for 15min, Blow and shake the centrifuge tube with a pipette every 5min or shake it gently for 1min, add 3ml DMEM medium containing 10% FBS to terminate digestion, centrifuge at 1400R/min for 5min, discard the supernatant, resuspend the cell precipitation with DMEM medium containing 10% FBS to 4ml, inoculate it into a culture bottle coated with FN mucin(F8180;solarbio) in in advance and culture for 0.5h, Then, the medium and non adherent cells are transferred to a new culture bottle coated with FN mucin for culture for 1h, and then the medium and non adherent cells are transferred to a new culture bottle coated with FN mucin for culture for 1H, Then, the culture medium and non adherent cells were transferred to a new culture bottle coated with FN mucin in advance, and the solution was changed after 72 hours of culture.

Histological analysis using hematoxylin-eosin (H&E) and Masson’s trichrome staining

Irradiated and control rectus femoris muscle tissues were fixed in 4% formaldehyde for 24 h, and paraffin-embedded biopsy sections were prepared. After dewaxing, the sections were stained with H&E (G1120; Solarbio) and Masson’s trichrome (BA-40798; Baso). An inverted microscope (Axio Scope A1; Zeiss) was used to observe all visual fields in each section, and the percentage of fibrotic area (collagen) was analyzed using the Image-Pro Plus 6 software (Media Cybernetics, Rockville, MD, USA).

TUNEL staining

All muscle tissues were fixed in 4% paraformaldehyde solution for 24 hours and embedded in paraffin μM thick slice. TUNEL was used to detect apoptosis with in situ cell death detection kit (11684817910; Roche), according to the manufacturer’s protocol. The sections were deparaffinized and permeabilized with proteinase K, incubated with a mixture of nucleotides and TdT enzyme solution at 37°C for 1 h, and then stained with DAPI. TUNEL-positive cells were imaged using an EVOS fluorescence microscope (AMG). Then, the cells were observed under an inverted fluorescence microscope (Axio Scope A1; Zeiss) at a magnification of 200× in a blinded manner. Cells emitting green fluorescence were considered apoptotic cells.

ELISA

IL-1β concentrations in the muscle and serum samples were determined using an ELISA kit (70-EK301B; Multi Sciences). A standard curve was drawn using a rat standard material included in the kit.

Immunofluorescence staining

SCs from the control and 90 Gy-4w groups were fixed in 4% formaldehyde solution at room temperature overnight, embedded in paraffin, and cut into 4-μm sections that were permeabilized with 0.1% Triton X-100 in PBS at room temperature for 15 min, blocked with 3% BSA for 15 min, and co-incubated with monoclonal rabbit anti-Pax7 antibody (sc-81648, 1:500 dilution) and monoclonal rabbit anti-Ki67 (GB13030-2; Servicebio, 1:500 dilution) at 4°C overnight. Then, the sections were incubated with goat anti-rabbit IgG conjugated to FITC (GB22303; Servicebio, 1:200 dilution). Nuclei were counterstained with DAPI (G1012; Servicebio). Images were captured using an inverted microscope (Axio Scope A1).

After the differentiation culture of 90Gy-4w SCs and L6 for 7 days, suck the culture medium, wash the six well plate or twelve well plate with PBS at 37℃ for 3-5s each time, gently suck the PBS dry, then add 4% paraformaldehyde to each well, fix it for 15 minutes and discard it, then add PBS to each well, shake and wash it on the decolorization shaking table for 3 times for 5 minutes each time. Drip 0.5% Triton into each hole, penetrate for 15min, and gently suck dry Triton. Then add PBS into each well, shake and wash on the decolorization shaking table for 3 times, each time for 5min. Goat serum was added dropwise for blocking and incubated for 30 min to remove. And incubated with primary antibodies, including

monoclonal rabbit anti-Pax7 antibody (sc-81648; Santa Cruz, 1:500 dilution) and monoclonal rabbit anti-MyHC antibody (sc-376157; Santa Cruz, 1:500 dilution) at 4°C overnight, followed by incubation with goat anti-rabbit IgG conjugated to FITC (GB22303; Servicebio,1:200 dilution). Nuclei were counterstained with DAPI(G1012; Servicebio).

Electron microscopy

Place the muscle in the sterile culture dish with dripping electron microscope fixing solution, cut it into small particles of about 1mm3 with a sharp blade, clamp it gently with tweezers (extrusion is prohibited), and quickly place it in the cryopreservation tube containing electron microscope fixing solution, and store it in the refrigerator at -4℃. These samples were fixed with 2.5% glutaraldehyde overnight, post-fixed in 1% osmium tetroxide for 2 h, dehydrated in a graded ethanol series, and embedded in Araldite. The ultrastructures of muscle fibers, skeletal muscle cells, and organelles were observed using a Tecnai G2 Spirit electron microscope (FEI, Hillsboro, OR, USA). The images were taken using the GATAN ORIUS CCD camera (GATAN, Pleasanton, CA, USA).

Statistical analysis

All experimental data were from at least three biological replicates. The data were expressed as the mean ± standard error (SEM) of the mean value, and SPSS software (version 25.0; SPSS, Chicago, Illinois, USA). Student t-test was used to compare the mean values of the two groups, and one-way ANOVA was used to compare the mean values of multiple groups, $p < 0.05$ indicating a statistically significant difference.

Results

Fibrosis increases over time following irradiation

To investigate fibrosis, irradiated muscles from rats with radiation-induced muscle fibrosis and muscles from control rats were stained with Masson's trichrome stain. In the control group (no radiation exposure), collagen fibers were hardly visible (Fig. 1A). In the 90 Gy-1 w and 90 Gy-2 w groups (i.e., at 1 and 2 weeks post irradiation, respectively), the amount of collagen fibers was slightly increased (Fig. 1B, C,). In the 90 Gy-4 w, 90 Gy-12 w, and 90 Gy-24 w groups (i.e., at 4, 12, and 24 weeks post irradiation, respectively), large amounts of collagen fibers were accumulated between the muscle fibers (Fig. 1D, E, F).

Irradiation induces apoptosis

To assess apoptosis, irradiated muscles from rats with radiation-induced muscle fibrosis and muscles from control rats were stained using TUNEL staining and observed using fluorescence microscopy. Representative photomicrographs from tissues of rats of each group are shown in Fig. 2A. In the control group, only a few apoptotic cells were observed. In the 90 Gy-4 w group, the number of apoptotic cells was significantly increased compared to that in the control group (Fig. 2A, B).

IL-1β protein concentrations in irradiated muscle and serum samples from rats with radiation-induced muscle fibrosis and corresponding samples from control rats were analyzed using ELISA. Compared with those in the control group, serum and muscle IL-1β concentrations were significantly increased in the 90 Gy-1 w, 90 Gy-2 w, 90 Gy-4 w, and 90 Gy-12 w groups (Fig. 2C, D), whereas there was no difference in the 90Gy-24w group.

Irradiation activates SCs

Pax7 is a marker commonly used for identifying SCs in myofibers(27). Irradiated muscles from rats with radiation-induced muscle fibrosis and muscles from control rats were subjected to immunofluorescence staining of pax7 and observed by fluorescence microscopy. Representative photomicrographs from tissues of rats of each group are shown in Fig. 3A. In the control group, $pax7^+$ cells were rare. In the 90 Gy-4 w group, the number of $pax7^+$ cells was increased. The number of $pax7^+$ cells, percentage of $pax7^+/DAPI^+$ cells, and percentage of $pax7^+/Ki67^+$cells were significantly increased in the 90 Gy-4 w group when compared with those in the control group (Fig. 3B).

Irradiation induces autophagy

Muscle samples from rats of all groups were examined using transmission electron microscopy. In the control group, muscle filaments were arranged neatly (Fig. 4A), mitochondria had well-structured cristae (Fig. 4B), and nuclei were normal and regular (Fig. 4C). In the 90 Gy-4 w group, muscle filaments were dissolved (Fig. 4D), nuclei were swollen (Fig. 4D), a few autophagic vacuoles were formed (Fig. 4E, F), and mitochondria were swollen, with widened cristae (Fig. 4E, F).

Irradiation induces the formation of central nuclear muscle fibers

Muscle samples from rats of all groups were assessed using H&E staining. In the control group, all myocytes were arranged orderly and their morphology was normal, and there were no centralized nuclei in the muscle fibers (Fig. 5A). In the 90 Gy-1 w group, myocytes were swollen and arranged disorderly, some muscle fibers were fractured, there was limited fibrous tissue deposition, and a limited amount of centralized nuclei were observed in the muscle fibers (Fig. 5B). In the 90 Gy-2 w and 90 Gy-4 w groups, myocytes were more swollen and arranged disorderly, and there were numerous fractured muscle fibers, substantial fibrous tissue deposition, substantial inflammatory cell infiltration, and a limited amount of centralized nuclei in the muscle fibers (Fig. 5C, D). In the 90 Gy-12 w group, myocytes were arranged disorderly, with substantial fibrous tissue deposition and some centralized nuclei in the muscle fibers (Fig. 5E). In the 90 Gy-24 w group, myocytes were arranged disorderly and had abnormal morphology, substantial fibrous tissue deposition, and numerous centralized nuclei in the muscle fibers (Fig. 5F). Centralized nuclei in the muscle fibers are a histological feature of muscle regeneration, and the percentage of central nuclear muscle fibers was significantly increased in all irradiated groups when compared to the control group (Fig. 5G).

Proliferation and differentiation of SCs from rats with radiation-induced muscle fibrosis

SCs were isolated from the irradiated muscles of the rats with radiation-induced muscle fibrosis. Cultured SCs had a spindle shape (Fig. 6A–C). MyHC is a commonly used marker for identifying myogenic differentiation(28). Cultured L6 cells and cultured SCs from irradiated muscles were positive for Pax7 (Fig. 6D, E). Myogenically differentiated L6 cells and myogenically differentiated SCs from irradiated muscles were positive for MyHC (Fig. 6F, G).Proliferation and differentiation of SCs from irradiated muscles was not altered by irradiation.

Discussion

Radiation-induced muscle fibrosis is a late-stage complication of radiotherapy. Muscle fibrosis and regeneration are two different processes, but fibrosis formation may be associated with regeneration(29). This study demonstrated that apoptosis and autophagy are both activated in rats with radiation-induced muscle fibrosis and to provide cellular evidence of SC activation in this model. Further, this study revealed that radiation does not significantly harm the proliferation and differentiation potential of SCs *in vitro*.

Under physiological conditions, muscle fibrosis and regeneration are balanced. In pathological conditions, permanent fibrosis prevents regeneration(30), and fibrotic tissue deposition is due to impaired muscle regeneration(31). Fibrosis deposition after irradiation is progressive and irreversible. Husu *et al.* used a fractionated high-dose irradiation-induced muscle damage rat model and found increased collagen deposition even 12 months post irradiation(32). The mechanism underlying the relationship between fibrosis and regeneration is complex. Various modes of radiation-induced cell death have been reported, including apoptosis, autophagy, mitotic catastrophe, and senescence-like cell death(33). Apoptosis has been observed in a mouse model of radiation-induced lung injury(34). Yang et al. found that apoptosis was significantly activated in a radiation-induced brain injury juvenile rat model(35). Both apoptosis and autophagy can be induced by irradiation, and cell fate depends on the balance between them. In a radiation-induced acute cerebral endothelial damage zebrafish larvae model, endothelial autophagy was strongly activated(36). Enhanced autophagy protects neurons from radiation-induced apoptosis(37). Autophagy inhibition by *ATG7* knockdown significantly increased radiation-induced neural stem cell apoptosis(38). Our data showed that apoptosis and autophagy were both activated upon irradiation. However, the detailed relationship and underlying mechanisms have not been elucidated. In addition to direct DNA damage, cytokines and inflammatory factors can cause apoptosis. Pro-inflammatory cytokines, such as IL-1, IL-6, and tumor necrosis factor (TNF)-α, cause an early inflammatory response to radiation(39). In a rat model of radiation-induced submental muscle injury, the expression of TGF-1β, MMP-2, and IL-6 was upregulated(40). IL-1β plays an important role in radiation-induced skin fibrosis(41). IL-1β has been shown to induce epithelial-to-mesenchymal transition in renal tubular and hepatic stellate cells(42)and apoptosis in chondrocytes *in vitro*(43). Our data showed that IL-

1β levels were increased in the irradiated groups; however, the mechanism of IL-1β-induced apoptosis was not revealed.

The healing process of injured skeletal muscle can be divided into four phases: degeneration, inflammation, regeneration, and maturation(44). Inflammatory cells and cytokines play vital roles in muscle regeneration. We previously showed that lymphocytes and macrophages are the main infiltrating inflammatory cells in irradiated tissues(45). Th1 cells produce IL-1, IL-2, TNF-α, and IFN-γ, whereas Th2 cells produce IL-4, IL-13, and IL-6(46). Two subpopulations of macrophages may influence muscle regeneration: M1 macrophages secrete pro-inflammatory cytokines, such as TNF-α, IL-1β, and IL-6, whereas M2 macrophages secrete anti-inflammatory cytokines, such as IL-10(47). IL-10 promotes the switch from M1 to M2 macrophages and induces SC proliferation-mediated muscle regeneration(48). Macrophages enhance the proliferation of myoblasts both *in vitro* and *in vivo*(49). IFN-γ inhibits SC proliferation and differentiation(50). IL-6 stimulates SC proliferation through STAT3 activation(51). In this study, we found that SCs were activated and central nuclear muscle fibers were formed in rats with radiation-induced muscle fibrosis. These findings suggest that activated SCs are a source of muscle regeneration and that exogenous administration of cytokines such as HGF and IGF-I to promote the proliferation and differentiation of SCs may be a good approach to treat radiation-induced muscle fibrosis. Furthermore, since radiation led to an increase in IL-1β levels, we speculate that promoting SC-mediated muscle regeneration by inhibiting IL-1β also may be useful to treat radiation-induced muscle fibrosis.

This study revealed the activation of autophagy and SC upon irradiation, but did not reveal the role of autophagy in SC activation nor the relationship between autophagy and SC activation in irradiation-induced muscle fibrosis. In future, we will use transgenic technology to clarify the role of autophagy in SC activation to provide a basis for further research on muscle regeneration.

Conclusion

We found that both apoptosis and autophagy were activated in a rat model of radiation-induced muscle fibrosis. In addition, SCs were activated, and central nuclear muscle fibers were formed *in vivo* following irradiation. Radiation did not significantly affect the proliferation and differentiation potential of SCs *in vitro*. Our results provide cellular evidence of SC activation and proliferation in the radiation-induced muscle fibrosis model.

Abbreviations

ELISA
enzyme linked immunosorbent assay;IL:interleukin; FBS:fetal bovine serum; DMEM:Dulbecco's modified Eagle's medium; TNF:tumor necrosis factor;FN:fibronectin.

Declarations

Acknowledgments

The authors acknowledge Zichao Ma, Bo Liang for valuable advice and help, the Animal Laboratory of Hunan Cancer Hospital and The Affiliated Cancer Hospital of Xiangya School of Medicine (Central South University, Changsha, Hunan, China) for providing the animal experimental setup and platform, and the electron microscopy facility at the Institute of Neuroscience, Chinese Academy of Sciences, for assistance with electron microscopy experiments.

Authors' contributions

XLZ and LYX performed the experiments, analyzed data and edited the manuscript. YXG and SL performed the experiments and literature search. XWS conceived and designed the study, prepared the manuscript and figure. XZ designed the study and edited the manuscript. All authors read and approved the final manuscript.

Funding

This study was supported by the National Natural Science Foundation of China (Grant no. 81903262 and no. 82030056), The science and technology innovation Program of Hunan Province (2020SK51103).The Natural Science Foundation of Hunan

Province(2021JJ70027).Clinical Research Center For Wound Healing In Hunan Province(2018SK7005).

Availability of data and materials

The datasets used and/or analyzed during the current study are available from the corresponding author on reasonable request.

Ethics approval and consent to participate

Ethics approval was obtained from the Animal Ethics Committee of Hunan Cancer Hospital, the Affiliated Cancer Hospital of Xiangya School of Medicine, Central South University.

Consent for publication

Not applicable

Competing interests

The authors declare that they have no competing interests.

Author details

[1]Graduate Collaborative Training of Hunan Cancer Hospital, Hengyang Medical School, University of South China, Department of Head and Neck Surgery, Central laboratory, The Affiliated Cancer Hospital of

Xiangya School of Medicine, Changsha, Hunan Province, China. [2]Changsha Medical University, Changsha, Hunan Province, China. [3]Department of Radiation Oncology, Hunan Cancer Hospital and The Affiliated Cancer Hospital of Xiangya School of Medicine, Central South University, Changsha, Hunan Province, China. [4]Nursing Department, Hunan Cancer Hospital and The Affiliated Cancer Hospital of Xiangya School of Medicine, Changsha, Hunan Province, China. [5]Institute of Neuroscience, Chinese Academy of Sciences, Shanghai, China. [6]Pathology Department, Hunan Cancer Hospital and The Affiliated Cancer Hospital of Xiangya School of Medicine, Changsha, Hunan Province, China. [7]Institute of Rocket Force Medicine, State Key Laboratory of Trauma, Burns and Combined Injury, Third Military Medical University, Chongqing, China.

References

1. Hawke T, Garry DJJoap. Myogenic satellite cells: physiology to molecular biology. 2001;91(2):534–51.
2. Zhou Y, Sheng X, Deng F, Wang H, Shen L, Zeng Y, et al. Radiation-induced muscle fibrosis rat model: establishment valuation. 2018;13(1):160.
3. Nicolas A, Dumont C, Florian. Bentzinger, et al. Satellite Cells and Skeletal Muscle Regeneration. 2015.
4. Yin H, Price F, Rudnicki MJPr. Satellite cells the muscle stem cell niche. 2013;93(1):23–67.
5. MAURO AJTJob, cytology b. Satellite cell of skeletal muscle fibers. 1961;9:493–5.
6. Collins C, Olsen I, Zammit P, Heslop L, Petrie A, Partridge T, et al. Stem cell function, self-renewal, and behavioral heterogeneity of cells from the adult muscle satellite cell niche. 2005;122(2):289–301.
7. Day K, Shefer G, Richardson J, Enikolopov G, Yablonka-Reuveni, ZJDb. Nestin-GFP reporter expression defines the quiescent state of skeletal muscle satellite cells. 2007;304(1):246–59.
8. Kuang S, Rudnicki MAJTiMM. The emerging biology of satellite cells and their therapeutic potential. 2008;14(2):82–91.
9. Brack AS, Rando TAJCSC. Tissue-Specific Stem Cells: Lessons from the Skeletal Muscle. Satellite Cell. 2012;10(5):504–14.
10. Philippou A, Barton ERJGH. Society IROJotGHR, Society tIIR. Optimizing IGF-I for skeletal muscle therapeutics. 2014;24(5):157–63.
11. Tatsumi R, Anderson JE, Nevoret CJ, Halevy O, Allen REJDB. HGF/SF is present in normal adult skeletal muscle and is capable of activating satellite cells. 1998;194(1):114–28.
12. Srikuea R, Hirunsai MJJoAP. Effects of intramuscular administration of 1α,25(OH)2D3during skeletal muscle regeneration on regenerative capacity, muscular fibrosis, and angiogenesis. 2016;120(12):1381–93.
13. Rosenblatt J, Lunt A, Parry D, Partridge, TJIvc. Animal db. Culturing satellite cells from living single muscle fiber explants. 1995;31(10):773–9.

14. Gromova A, Tierney MT, Sacco AJBP. FACS-based Satellite Cell Isolation From Mouse Hind Limb Muscles. 2015;5(16).
15. Blau HM, Webster CJPotNAoS. Isolation and characterization of human muscle cells. 1981;78(9):5623-7.
16. Yablonka-Reuveni. ZJMr, technique. Development and postnatal regulation of adult myoblasts. 1995;30(5):366–80.
17. Bo-jiang, Li Ping-hua, Li Rui-hua. Huang, et al. Isolation, Culture and Identification of Porcine Skeletal Muscle Satellite Cells. 2015;28(8).
18. Biressi S. Rando TJSic, biology d. Heterogeneity in the muscle satellite cell population. 2010;21(8):845–54.
19. Ding S, Wang F, Liu Y, Li S, Zhou G, Hu PJCDD. Characterization and isolation of highly purified porcine satellite cells. 2017;3:17003.
20. Schaaf G, Canibano-Fraile R, van Gestel T, van der Ploeg A. Pijnappel WJAotm. Restoring the regenerative balance in neuromuscular disorders: satellite cell activation as therapeutic target in Pompe disease. 2019;7(13):280.
21. Lee S, Du J, Stitham J, Atteya G, Lee S, Xiang Y, et al. Inducing mitophagy in diabetic platelets protects against severe oxidative stress. 2016;8(7):779–95.
22. White JP, Billin AN, Campbell ME, Russell AJ, Huffman KM, Kraus WEJSCR. The AMPK/p27 Kip1 Axis Regulates Autophagy/Apoptosis Decisions in Aged Skeletal Muscle Stem Cells. 2018:S2213671118302777-.
23. Garcia-Prat L, Martinez-Vicente M, Perdiguero E, Ortet L, Rodriguez-Ubreva J, Rebollo E, et al. Autophagy maintains stemness by preventing senescence. 2016;529(7607):37–42.
24. Tang AH, Rando TAJEJ. Induction of autophagy supports the bioenergetic demands of quiescent muscle stem cell activation. 2015;33(23):2782–97.
25. Ryall J, Dell'Orso S, Derfoul A, Juan A, Zare H, Feng X, et al. The NAD(+)-dependent SIRT1 deacetylase translates a metabolic switch into regulatory epigenetics in skeletal muscle stem cells. 2015;16(2):171–83.
26. Silvia Z, Matteo G, Cristiana P, Federica M, Thierry T, Di RI, et al. Autophagy controls neonatal myogenesis by regulating the GH-IGF1 system through a NFE2L2- and DDIT3-mediated mechanism. 2018:15548627.2018.1507439-.
27. Feng X, Naz F, Juan AH, Dell'Orso S, Sartorelli VJJoVE. Identification of Skeletal Muscle Satellite Cells by Immunofluorescence with Pax7 and Laminin Antibodies. 2018;2018(134).
28. Zammit PS, Partridge TA, Yablonka-Reuveni ZJJoH. Society COJotH. The skeletal muscle satellite cell: the stem cell that came in from the cold. 2006;54(11):1177–91.
29. Garg K, Corona BT, Walters TJJFiP. Therapeutic strategies for preventing skeletal muscle fibrosis after injury. 2015;6:87.

30. Uezumi A, Ito T, Morikawa D, Shimizu N, Yoneda T, Segawa M, et al. Fibrosis and adipogenesis originate from a common mesenchymal progenitor in skeletal muscle. 2011;124(21):3654–64.
31. Mahdy MJC, Research T. Skeletal muscle fibrosis: an overview. 2019;375(3):575–88.
32. Hsu H, Chai C, Lee MJRr. Radiation-induced muscle damage in rats after fractionated high-dose irradiation. 1998;149(5):482–6.
33. Kondo TJNrJjocm. [Radiation-induced cell death]. 2012;70(3):389–93.
34. Zhang Y, Zhang X, Rabbani ZN, Jackson IL, Vujaskovic ZJIJoROBP. Oxidative stress mediates radiation lung injury by inducing apoptosis. 2012;83(2).
35. Yang J, Gao J, Han D, Li Q, Oncology YLJR. Hippocampal changes in inflammasomes, apoptosis, and MEMRI after radiation-induced brain injury in juvenile rats. 2020;15(1).
36. Ai X, Ye Z, Yao Y, Xiao J, Zhao CJSR. Endothelial Autophagy: an Effective Target for Radiation-induced Cerebral. Capillary Damage. 2020;10(1):614.
37. Zhang L, Huang P, Tian Y, Yang HJIJoROBP. The Inhibitory Effect of Minocycline on Radiation-Induced Neuronal Apoptosis Via AMPKα1. Signaling-Mediated Autophagy. 2017;99(2):E631.
38. Wsa B, Wei L, Jma B, Jla B, Xy D, Jw D, et al. The role of Atg7-mediated autophagy in ionizing radiation-induced neural stem cell damage.738.
39. Salvo N, Barnes E, Van DJ, Stacey E, Mitera G, Breen D, et al. Prophylaxis and management of acute radiation-induced skin reactions: a systematic review of the literature. 2010;17(4):94–112.
40. King SN, Al-Quran Z, Hurley J, Wang B, Dunlap N. Cytokine and Growth Factor Response in a Rat Model of Radiation Induced Injury to the Submental Muscles. 2019.
41. Liu W, Ding I, Chen K, Olschowka J, Okunieff PJRR. Interleukin 1β (IL1B) Signaling is a Critical Component of Radiation-Induced. Skin Fibrosis. 2006;165(2):181.
42. Masola V, Carraro A, Granata S, Signorini L, Bellin G, Violi P, et al. In vitro effects of interleukin (IL)-1 beta inhibition on the epithelial-to-mesenchymal transition (EMT) of renal tubular and hepatic stellate cells. 2019;17(1).
43. Wang L, Gai P, Xu R, Zheng Y, Lv S, Li Y, et al. Shikonin protects chondrocytes from interleukin-1beta-induced apoptosis by regulating PI3K/Akt signaling pathway. 2015;8(1):298–308.
44. Gurriarán-Rodríguez U, Santos-Zas I, González-Sánchez J, Beiroa D, Moresi V, Mosteiro CS, et al. Action of Obestatin in Skeletal Muscle Repair: Stem Cell Expansion, Muscle Growth, and Microenvironment Remodeling. 2015;23(6).
45. Sheng X, Zhou Y, Wang H, Shen Y, Liao Q, Rao Z, et al. Establishment and characterization of a radiation-induced dermatitis rat model. 2019.
46. Gordon, Immunology SJNR. Alternative activation of macrophages. 2003;3(1):23–35.
47. Wynn TA, Chawla A, Pollard JWJN. Macrophage biology in development, homeostasis and disease. 2013;496(7446):445–55.
48. Deng B, Wehling-Henricks M, Villalta SA, Wang Y, Tidball JGJJoI. IL-10 Triggers Changes in Macrophage Phenotype That Promote Muscle Growth and Regeneration. 2012;189(7):3669–80.

49. Cantini M, Giurisato E, Radu C, Tiozzo S, Pampinella F, Senigaglia D, et al. Macrophage-secreted myogenic factors: a promising tool for greatly enhancing the proliferative capacity of myoblasts in vitro and in vivo. 2002;23(4):189.
50. Villalta SA, Deng B, Rinaldi C, Wehling-Henricks M, Tidball JGJJoI. IFN-γ promotes muscle damage in the mdx mouse model of Duchenne muscular dystrophy by suppressing M2 macrophage activation and inhibiting muscle cell proliferation. 2011;187(10):5419–28.
51. Serrano AL, Baeza-Raja B, Perdiguero E, Jardí M, Metabolism PMO-CJC. Interleukin-6 is an essential regulator of satellite cell-mediated skeletal muscle hypertrophy. 2008;7(1):33–44.

Figures

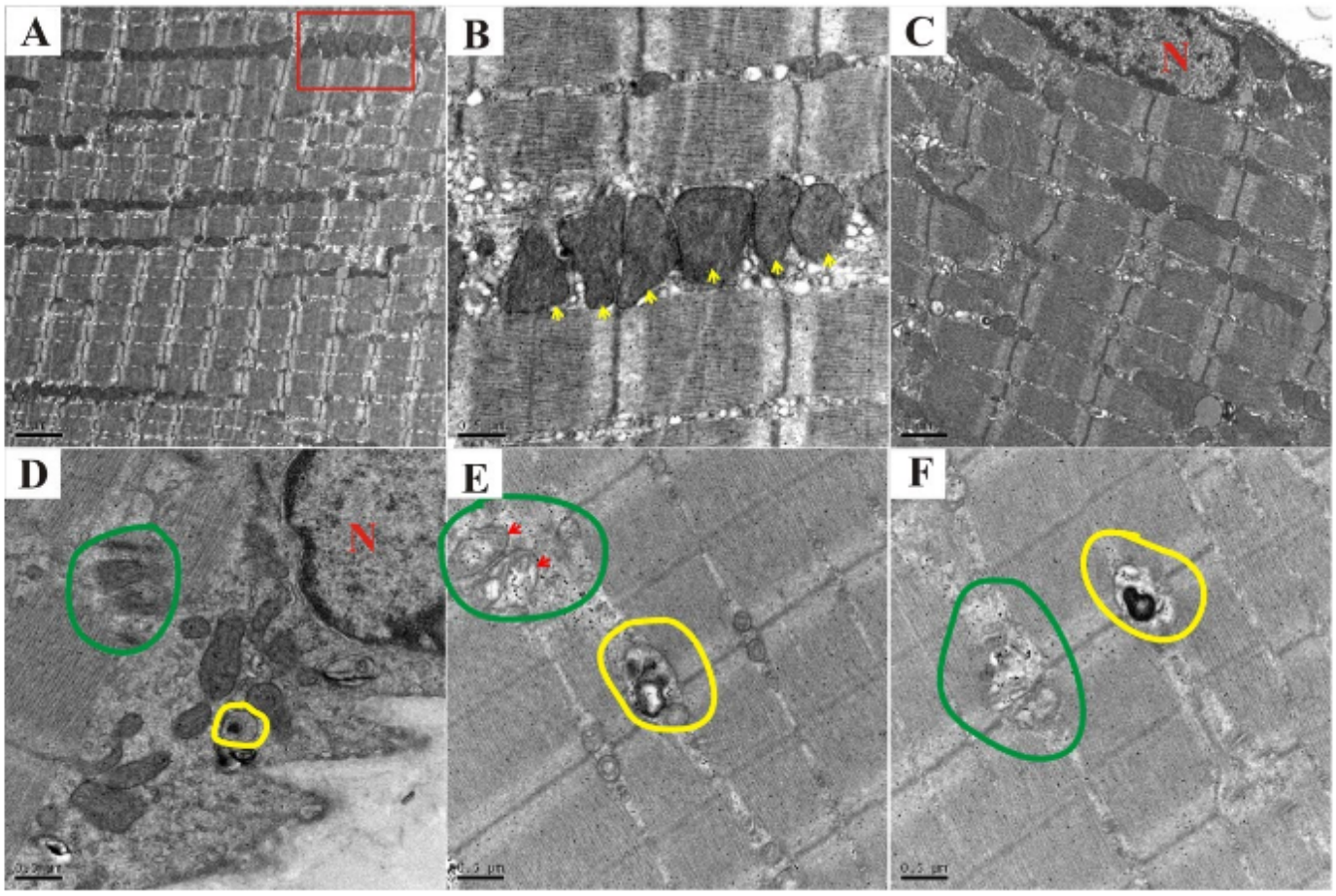

Figure 1

Representative photographs of Masson staining of irradiated muscles from rats of the control (A), 90 Gy-1 w (B), 90 Gy-2 w (C), 90 Gy-4 w (D), 90 Gy-12 w (E), and 90 Gy-24 w (F) groups.

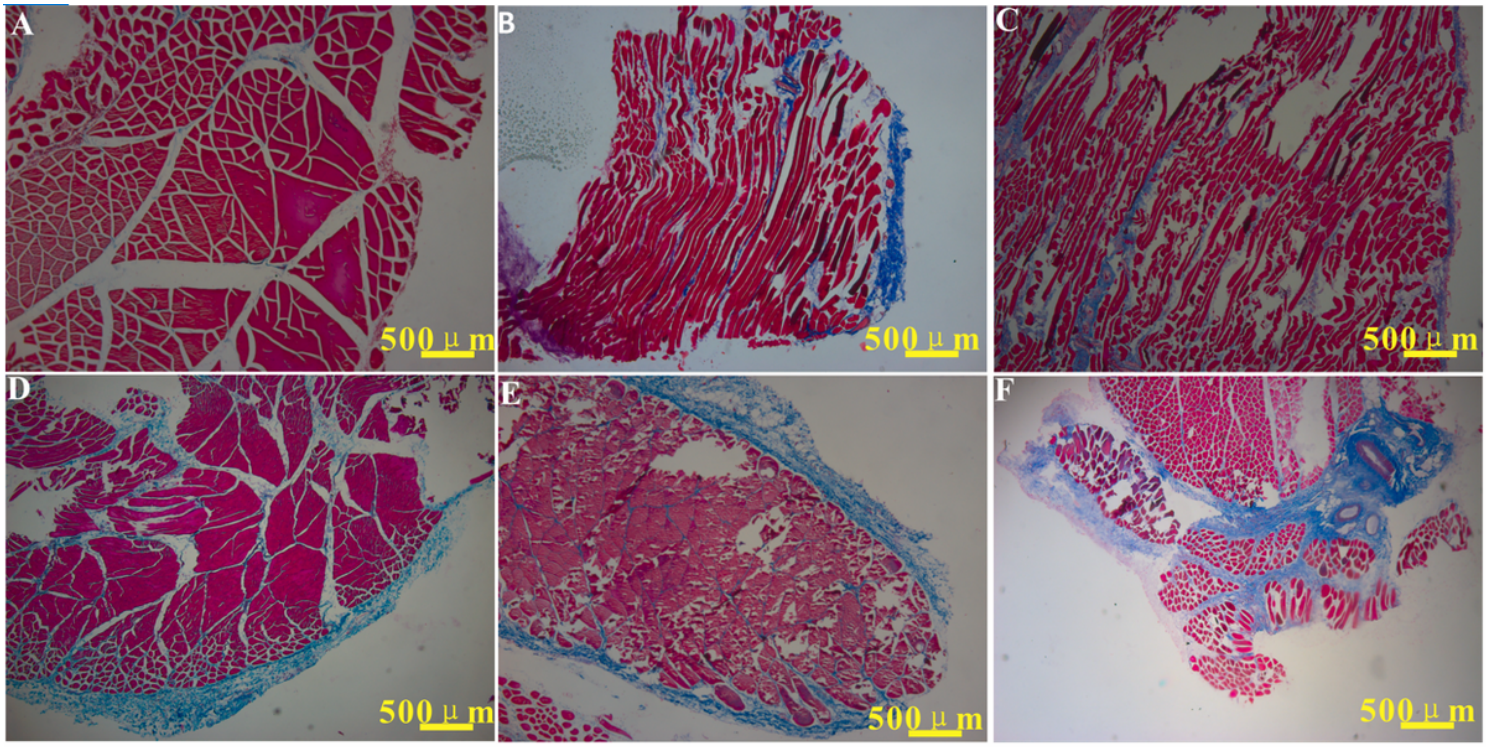

Figure 2

Apoptosis is activated in irradiated muscle. Representative images from rats of the control and 90 Gy-4 w groups (A). Nuclei of TUNEL-positive cells are stained green. Percentages of apoptotic cells were significantly higher in the 90 Gy-4 w group than in the control group. (B, n = 6/group). Serum IL-1β protein concentrations in rats of the control, 90 Gy-1 w, 90 Gy-2 w, 90 Gy-4 w, 90 Gy-12 w, and 90 Gy-24 w groups (C, n = 3/group). Muscle IL-1β protein concentrations in all groups (D, n = 3/group). The results are expressed as the mean ± SEM. *p < 0.05, **p < 0.01,***p < 0.001 vs. the control group.

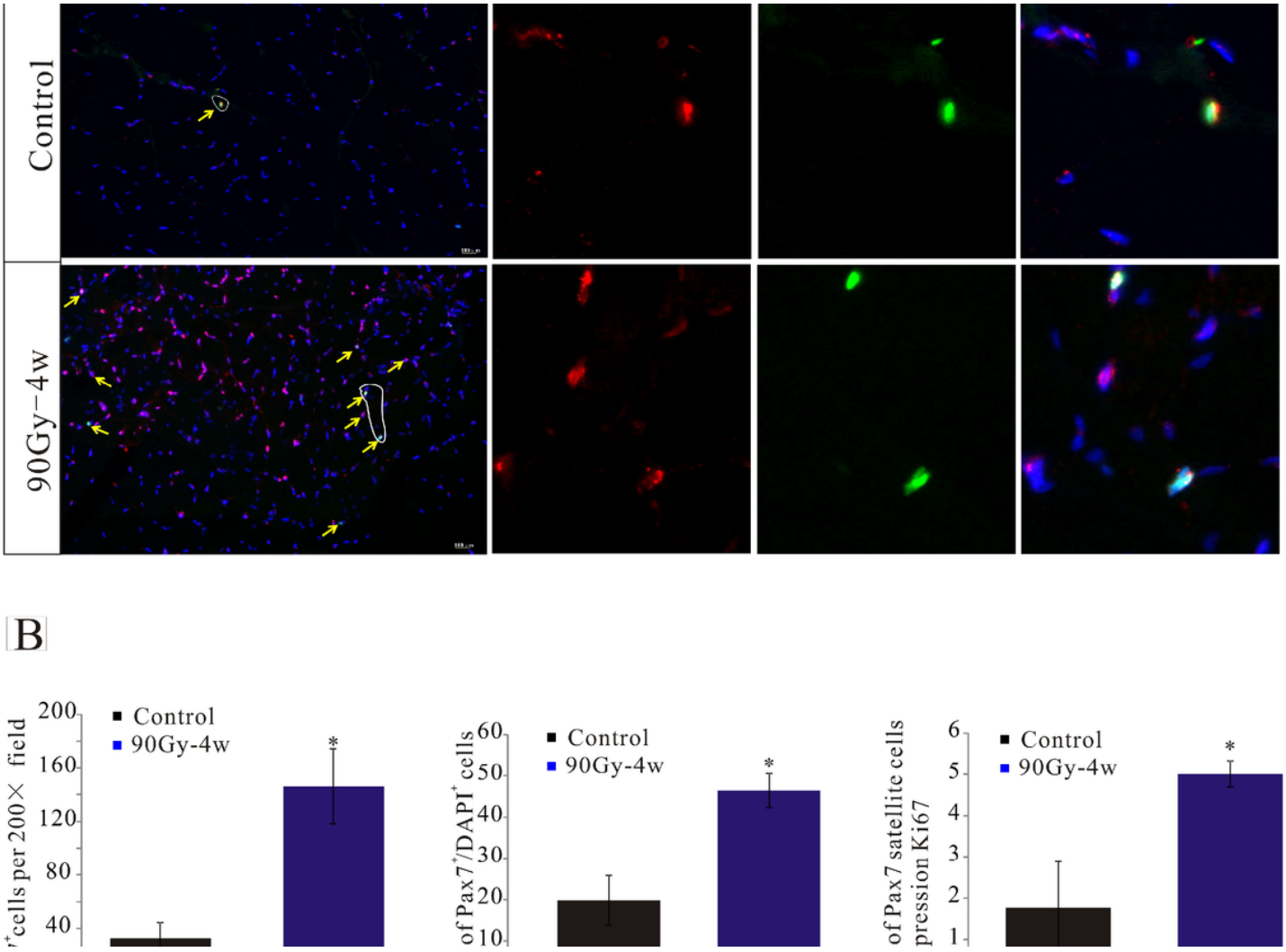

Figure 3

SCs are activated in irradiated muscle. Representative photographs of immunofluorescence staining of rats of the control and 90 Gy-4 w groups (A). Pax7 + cells are stained red, Ki67+ cells are stained green. The number of pax7+ cells, the percentage of pax7+/DAPI+ cells, and the percentage of pax7+/Ki67+cells were analyzed in each group (B). The results are expressed as the mean ± SEM. *p < 0.05 vs. the control group

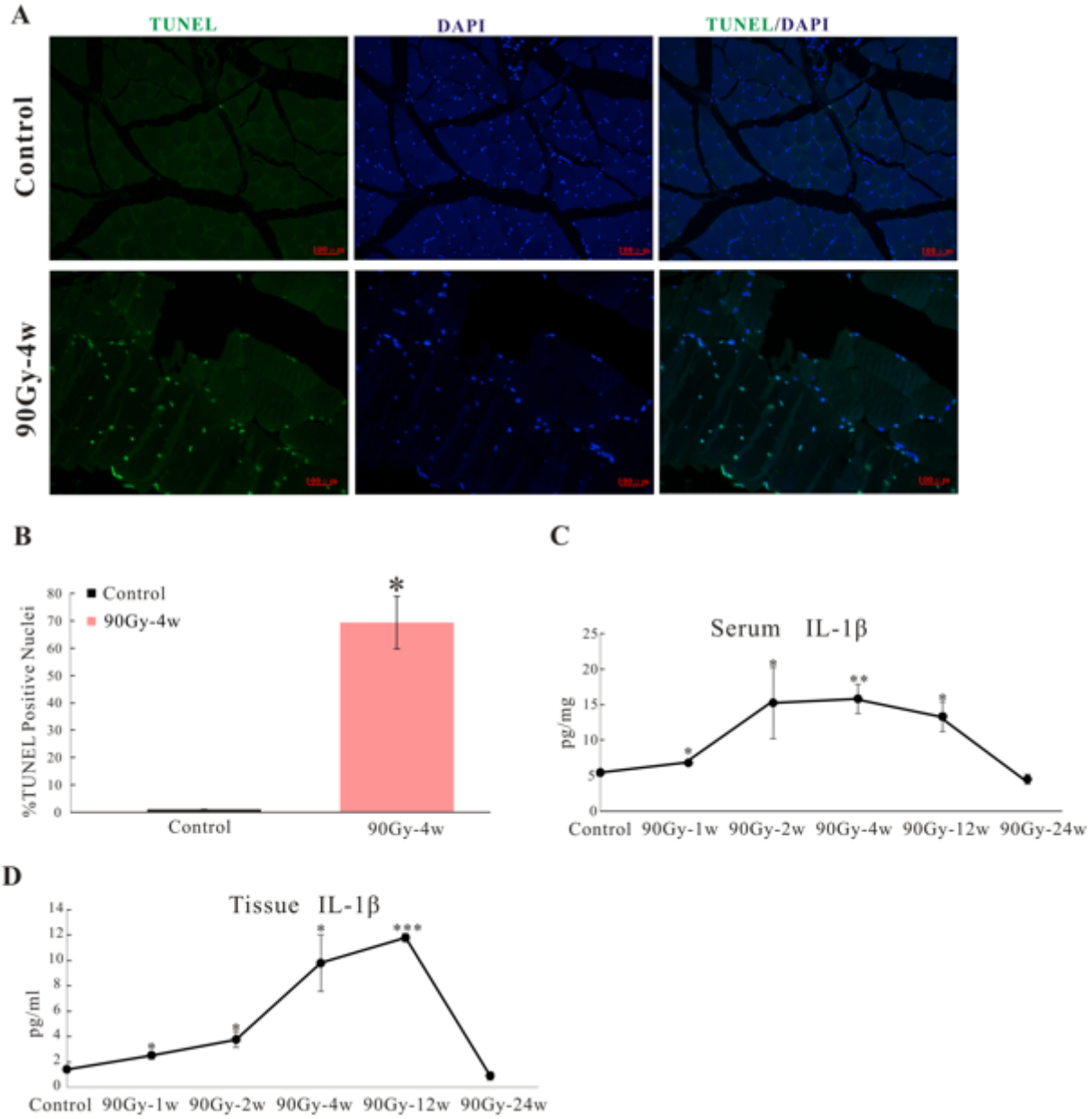

Figure 4

Transmission electron microscopic analysis of the ultrastructure of muscle tissues. Representative photographs showing the ultrastructure of muscle tissues in the control (A–C) and 90 Gy-4 w (D–F) groups. The red box and yellow arrows indicate regular mitochondria (A, B), and the red “N” indicates regular nuclei in the control group (C). The green circle indicates dissolved muscle filaments (D), yellow circles indicate autophagic vacuoles (D–F), green circles indicate damaged mitochondria with loss of cristae (E, F), and the red “N” indicates irregular nuclei in the 90 Gy-4 w group (D).

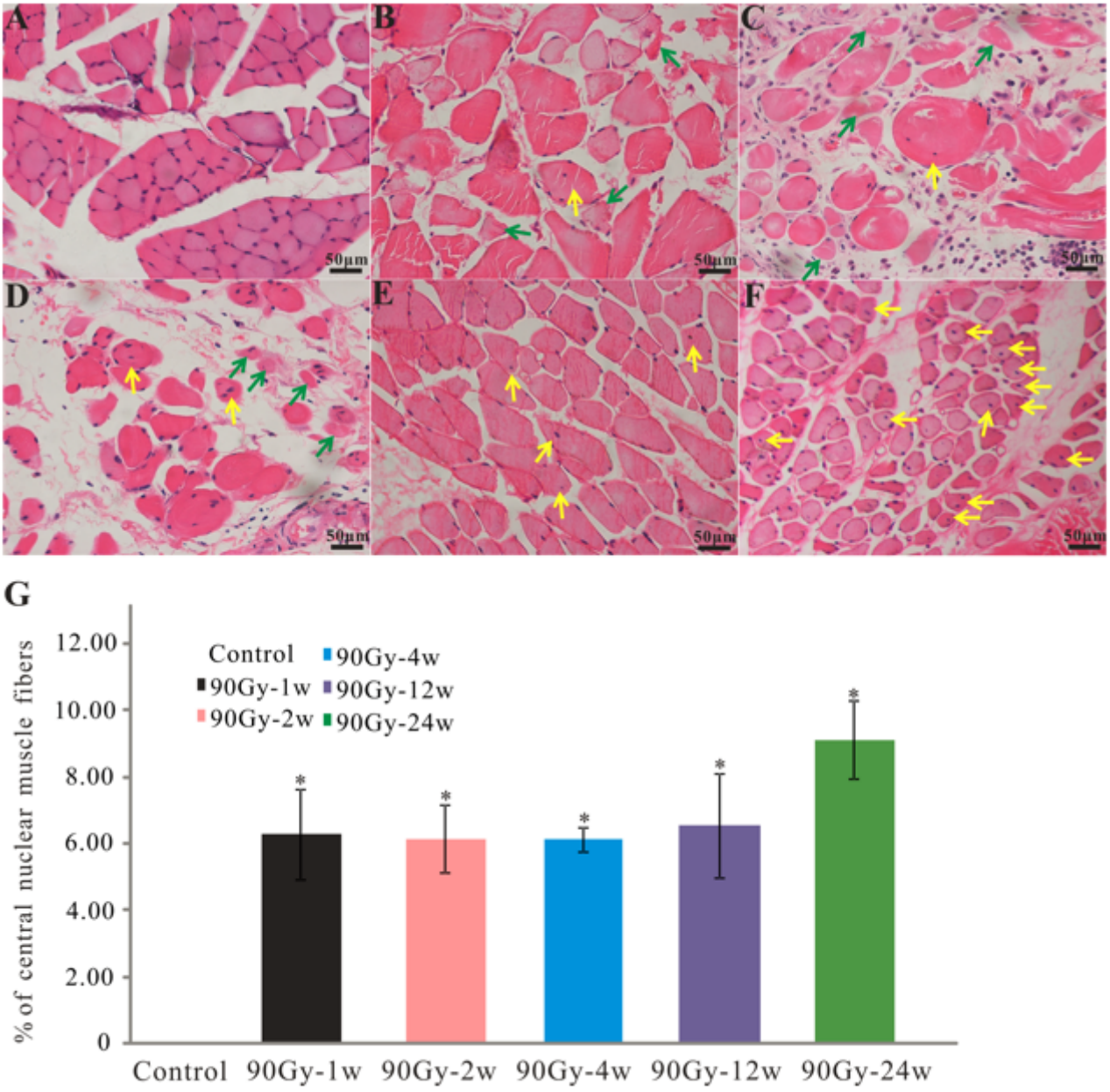

Figure 5

Central nuclear muscle fibers are formed following irradiation. Representative images of hematoxylin and eosin-stained muscles from rats of the control (A), 90 Gy-1 w (B), 90 Gy-2 w (C), 90 Gy-4 w (D), 90 Gy-12 w (E), and 90 Gy-24 w (F) groups. Yellow arrows indicate central nuclear muscle fibers (B–F) and green arrows indicate disrupted muscle fibers in the irradiated groups (B–D). Percentage of central nuclear muscle fibers compared with control group respectively (G). The results are expressed as the mean ± SEM. *$p < 0.05$ vs. the control group.

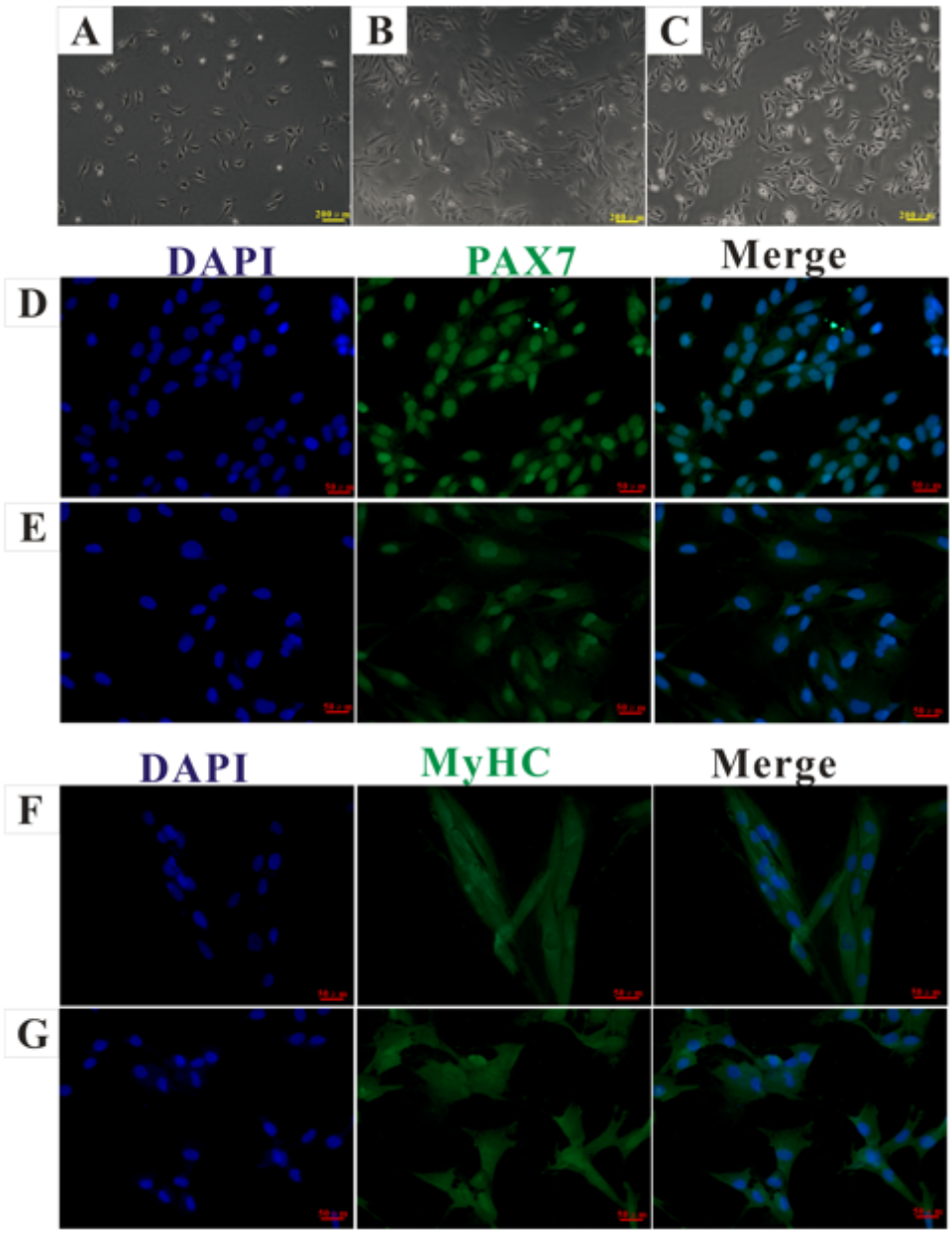

Figure 6

SCs isolated from irradiated muscles of rats with radiation-induced muscle fibrosis. Representative photographs of isolated and cultured SCs (A–C). Representative images of Pax7 immunofluorescence staining of cultured L6 cells (D) and SCs from irradiated muscle (E). Representative images of MyHC immunofluorescence staining of differentiated L6 cells (F) and SCs from irradiated muscle (G).